https://doi.org/10.5194/hess-2021-536
Preprint. Discussion started: 30 November 2021

Hydrology and Earth System Sciences
Discussions

Improving the understanding of N transport in rural catchments under Atlantic climate conditions from analysis of the concentration-discharge relationship derived from a high frequency data set

Rodríguez-Blanco, María Luz[1], Taboada-Castro, María Mercedes[2], Taboada-Castro, María Teresa[3]

[1]History, Art and Geography Department, GEAAT Group, University of Vigo, Campus As Lagoas, 36310 Ourense, Spain
[2]ETSIIAA, Area of Soil Science and Soil Chemistry, University of Valladolid, 34004 Palencia, Spain
[3]Faculty of Sciences, Centre for Advanced Scientific Research (CICA), University of A Coruna 15071 A Coruña, Spain

Correspondence to: M.L. Rodríguez-Blanco (maria.luz.rodriguez.blanco@uvigo.es)

Abstract. Understanding processes controlling stream nutrient dynamics over time is crucial for implementing effective management strategies to prevent water quality degradation. In this respect, the study of the nutrient concentration-discharge (C-Q) relationship during individual runoff events can be a valuable tool for extrapolating the hydrochemical processes controlling nutrient fluxes from streams. This study investigated nitrogen concentration dynamics during events by analyzing and interpreting the nitrogen C-Q relationship in a small Atlantic (NW Iberian Peninsula) rural catchment. To this end, nitrate (NO_3) and total Kjeldahl nitrogen (TKN) concentrations were monitored at high temporal resolution during 102 runoff events over a 6-year period. For each of the selected runoff events, C-Q response was examined visually for the presence and direction of hysteresis loops and classified into three types of responses: clockwise and anticlockwise and no hysteresis. Some metrics, such as the change in concentration (ΔC) and the overall dynamics of hysteresis loops (ΔR), were used to quantify nitrogen behavior during the runoff events. The results showed how transport mechanisms varied between parameters. The most frequent hysteretic response for NO_3 was enrichment with anticlockwise rotation, indicating that subsurface flow is the main pathway to the stream. On the contrary, the TKN dynamic was dominated by clockwise hysteresis, suggesting that surface runoff is mainly responsible for the transport of TKN to the river. Hysteresis direction (ΔR) and magnitude (ΔC) were better explained by event characteristics, such as rainfall, runoff, and discharge increase than by antecedent conditions (antecedent precipitation and baseflow).

Keywords: concentration-discharge, hysteresis, nitrogen, runoff events, rural catchment, Atlantic climate, NW Iberian Peninsula.

1 Introduction

Water is essential to life and, therefore, water resources are at the core of the development of societies and ecosystems. Nevertheless, anthropogenic activities have altered the natural state of this valuable resource, affecting the quantity and quality of water, as well as the health of the aquatic ecosystem (Meybeck, 2005; Vörösmarty et al., 2010; Abbot et al., 2019). Diffuse

https://doi.org/10.5194/hess-2021-536
Preprint. Discussion started: 30 November 2021

Hydrology and Earth System Sciences
Open Access
EGU
Discussions

nitrate water pollution is one of the most widespread environmental issues in the world, since it is the leading cause of pressure on freshwater quality (EEA, 2018).

In Europe, despite the advances made in the field of improving the environment quality of water bodies in recent decades, 60% of freshwaters fail to achieve good ecological status as established by the Water Framework Directive (Directive 2000/60/EC) (EEA, 2018). The European Directive urges Member States to monitor water quality. However, many Member States, Spain among them, have an inadequate water monitoring network to ensure a comprehensive and consistent monitoring of water bodies (EC, 2019). Moreover, water quality assessments historically have relied on routine low-frequency monitoring at main rivers, commonly every two weeks or at monthly resolution. This traditional sampling method can provide valuable information to identify sites that are under pressure due to anthropogenic activities, also to observe long-term trends in relation to land use, but cannot provide knowledge on nutrient dynamics under contrasting hydrological conditions, which is essential to develop suitable management programs to restore or maintain water quality (Bieroza et al., 2018). Therefore, there is an increasing interest in high-frequency water quality monitoring over the long term, which can be used to investigate nutrient behaviors, as this type of monitoring enables a broad range of nutrient concentrations in response to discharge to be captured (Bieroza et al., 2018; D'Amario et al., 2021).

High-frequency monitoring is particularly useful to better understand nutrient dynamics, which are more active during runoff events than during stable discharge conditions (low flow), due to changes in storage-flux interactions and transport pathways. Hence, the event-scale relationships between nutrient concentrations and discharge (C-Q) have been intensively investigated to better understand catchment nutrient functioning (Butturini et al., 2008; Ramos et al., 2015;Aguilera and Melack, 2018; Burns et al., 2019). The most commonly observed pattern in the C-Q relationship is the hysteresis loop, which reflects a non-linear solute or particulate behavior during runoff events as concentrations at a given discharge differ on the rising and falling limb of the hydrograph. The width, magnitude and direction of these loops have been used to investigate the sources, flow paths and transport mechanisms responsible for the export of nutrients from catchments. Generally, clockwise hysteresis is interpreted to reflect proximal and rapidly mobilized sources, whereas anticlockwise hysteresis reflects sources that are either proximal to the stream channel with slow transport, or those that are distal to the stream (Eludoyin et al., 2017; Baker and Showers 2019; Knapp et al., 2020). The C-Q relationship also results in positive or negative hysteresis slopes for stream water representing enrichment or dilution effects, respectively. Runoff events can also display complex hysteresis loops due to the spatial-temporal variability of rainfall, antecedent moisture conditions, etc. (Ramos et al., 2015)

For the most part, the nitrogen C-Q relationships have been examined on large rivers with high drainage basins and strongly impacted by pollution (e.g., (Cerro et al., 2014; Dupas et al., 2016; Outram et al., 2016)). These basins comprise several landscape types, with potentially different N paths that cannot be decoded solely by observations at the outlet of large basins. Only a few studies have analyzed the trajectories of N dynamics in relatively small but clean rural headwater catchments, despite the fact that catchment response (in temperate areas) to rainfall events is dominated by processes in headwater subcatchments. Consequently, accurate assessments of the complex processes of N dynamics in these systems are hindered by the limited availability of high-frequency data. This information is essential to anticipate changes in freshwater resources in compliance with the Water Framework Directive planning and monitoring norms. Therefore, it is necessary to provide new information on the issue to augment current studies across Europe and the Iberian Peninsula, in particular.

In this context, the aim of this study was to examine the N dynamics on a small Atlantic headwater catchment localized in NW Iberian Peninsula, using high-frequency measurements of nitrate (NO_3)· and total Kjeldahl nitrogen (TKN) during runoff events of contrasting magnitudes. More specifically, the objectives of this research were to: i) evaluate the dominant hysteresis patterns in NO_3 and TKN behavior and ii) identify hydrologic drivers that could potentially influence the main features of NO_3 and TKN hysteresis. The analysis of nitrogen C-Q relationship responses in Atlantic streams in Southwest Europe is still in a preliminary phase, and studies exploring these relationships in small rural Atlantic systems, like the study area, are becoming increasingly rare. In addition, studies including TKN are still scarcer because less attention has been paid to TKN behavior compared with NO_3, although some studies suggest that TKN contributions can be important and constitute a significant portion of the total nitrogen export (Hagedorn et al., 2000; Kaushal and Lewis 2003). In this way, this study provides a good example of the role of small temperate rural catchments in nitrogen dynamics. Moreover, the selected catchment (Corbeira, 16 km^2, NW Iberian Peninsula) is of particular interest, as it is a tributary of the Mero River, which discharges into the Abegondo-Cecebre reservoir - the main water supply for the city of A Coruña and surrounding municipalities (450 000 inhabitants) - and finally drains into the Atlantic Ocean through the ria of O Burgo. The Cecebre-Abegondo reservoir is a Natural 2000 EU site, classified as a Special Area of Conservation (ES1110004) in 2014 under the EU Habitats Directive (Directive 92/43/ECC) and one of the Core Zones of the Mariñas Coruñesas e Terras do Mandeo Biosphere Reserve, sustaining important bird, macroinvertebrate, and fish populations. Nevertheless, the ecological status of the Abegondo-Cecebre reservoir has deteriorated in the last few decades due to pollution, the presence of invasive alien species and fluctuations of river flow discharge (Ameijenda et al., 2010).

2 Material and methods

2.1 Study site

The study was conducted in a headwater catchment of 16 km^2 located in NW Spain, approximately 30 km southeast of the city of A Coruña (Galicia, NW Iberian Peninsula) (Fig. 1). The catchment is characterized by low drainage density (1.38 km km^{-2}), mean slope of 19% and a total relief of 410 m. The bedrock consists of basic schist of the Órdenes Complex (IGME, 1981) and the soils are predominantly Umbrisols and Cambisols (IUSS, 2015), with a silt and silty-loam texture, variable organic matter content (4.4-10.5%) and acid pH in the surface soil layer. The soils have a high infiltration capacity, so overland flow is unusual. Groundwater is the dominant source of water to the stream and the baseflow index is 0.75 (Rodríguez-Blanco, et al., 2012a). The catchment land cover consists of a mixture of forest (65%), agricultural fields (30%) and impervious areas (5%), consisting of roads and single-family homes that are not always connected to sewage disposal systems. Agricultural areas are dominated by pastures (26% of total area), the remaining agricultural area (4%) cultivates maize and winter cereals.

Organic and inorganic fertilizers are commonly used in agricultural areas throughout the year, including the wettest months. Forest areas are not fertilized. The annual N input to the catchment is approximately 37.8 kg N ha^{-1} (Rodríguez-Blanco et al., 2015), so nitrogen inputs in the Corbeira catchment can be considered low when compared to catchments with more intense agriculture.

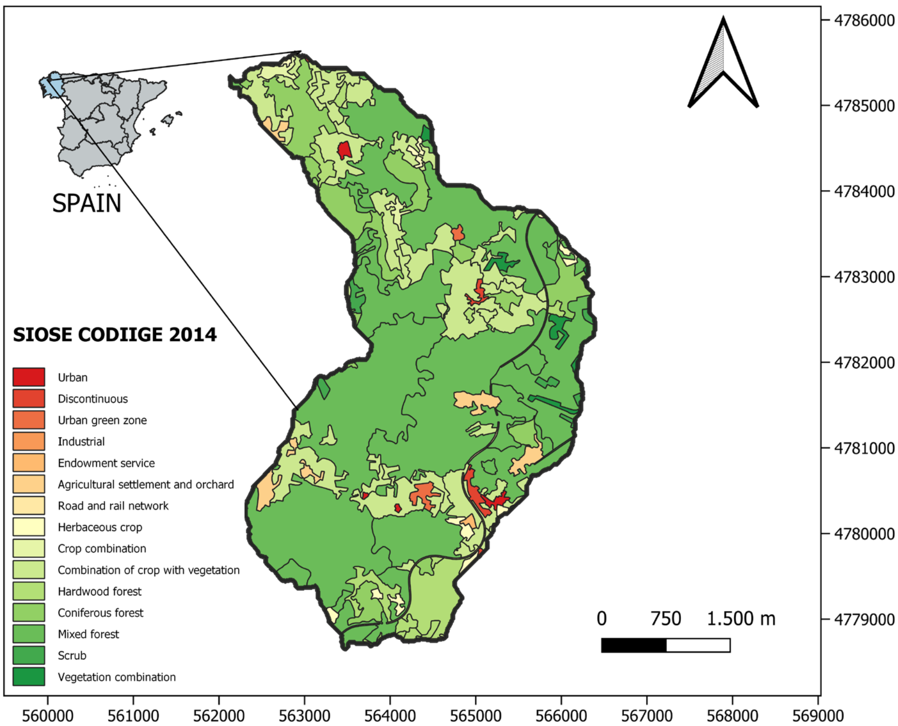

Figure 1: Location and land use of the Corbeira catchment.

The study area is located within the Eurosiberian biogeographic region, particularly in the Cantabrian-Atlantic province (Instituto Geográfico Nacional, 2008). It is included in the temperate oceanic climate region (Csb) according to Köppen-Geiger classification. Mean annual rainfall and temperature for the period 1983-2020 are 1075 mm and 13ºC, respectively (data from 10045 stations of the official meteorological service of the Galician Government-Meteogalicia, located near to the study catchment). The wettest period is from October to March, and the driest and hottest months are usually in summer (June-September). The hydrological regime is pluvial, with maximum discharge in December and low flows from June to September. Mean daily-recorded discharge is 0.18 m3 s-1. For more detailed information of the hydrological behavior of this catchment see (Rodríguez-Blanco et al., 2012b; 2020).

2.2 Data acquisition: monitoring, sampling, and water analysis

The research period comprised six hydrological years, during which rainfall, discharge, and N concentrations were measured. Rainfall was monitored at 10-min intervals using three rainfall gauges (0.2 mm resolution) distributed across the catchment. The Thiessen Polygon method (Linsey et al., 1949) was used to calculate the mean rainfall in the catchment. Water discharge was measured at 10-min resolution at the catchment outlet. A differential pressure transducer sensor (ISCO-720) coupled to an automatic water sampler (ISCO 6712-FS) recorded water level at 10-min resolution. The water level was then converted into discharge by rating-curve development over a wide range of discharge conditions at the sampling location.

Stream water samples were taken at the catchment outlet during runoff events using the automatic water sampler (Teledyne ISCO, Portable Sampler 6712-FS) fitted with 24 polypropylene 1-liter bottles. The pump inlet of the autosampler was placed near the pressure sensor. The sampler was programmed to start when the stream water level increased 2-3 cm above the level at the beginning of a rainfall event, and water samples were taken during the rising and recession limbs of the hydrograph to collect key runoff phases. The pumping frequency varied between 1-8 h depending on the magnitude and duration of the runoff events.

All water samples were stored in the dark and refrigerated at 4ºC until analyzed for the following parameters: electrical conductivity (EC), ammonium (NH_4^+), total Kjeldahl nitrogen (TKN), nitrate (NO_3) and nitrite (NO_2^-); $NH4^+$ was only analysed during the first six months of the study. Electrical conductivity at a reference temperature of 20 ºC was measured using a Crison conductivity meter. TKN concentrations were determined by Kjeldahl digestion of unfiltered samples according to the APHA method (APHA, 1998). After sample filtration (0.45 μm) NO_3 and NO_2 concentrations were analyzed by capillary electrophoresis, while NH_4 was measured using an ammonia-selective electrode. In this paper, only data concerning NO_3 and TKN are presented because the concentrations of NO_2 and NH_4 measured were below the detection limit (0.06 and 0.05 mg L^{-1}, respectively).

2.3 Selection of runoff events and description of C-Q hysteresis

The runoff events were defined as any hydrological response to rainfall which resulted in discharge increase equal to or higher than 1.5 times the discharge at the beginning of a rainfall event (the latter being defined as a rainfall episode following an interval of at least 10 hours with rain). The beginning of the runoff event was identified as an inflection point differentiating the start of the event from antecedent conditions. The end of a runoff event was identified as the point on the falling limb where discharge approached baseflow conditions or when another hydrological event commenced.

The events identified were characterized by three groups of variables: i) variables related to antecedent conditions (i.e., variables characterizing the conditions prior to the event), ii) event variables (rainfall and discharge) and iii) variables related to NO_3 and TKN concentrations (Table 1). Antecedent conditions were described by accumulated rainfall 7 and 15 days prior to the event (AP7d, and AP15d, respectively, mm), and the discharge at the beginning of the event (Qb, m^3 s^{-1}). Event variables included rainfall amount (P, mm); maximum 10-min rainfall intensity (IP10, mm h^{-1}); rainfall kinetic energy (KE, MJ ha^{-1}), peak discharge (Qmax, m^3 s^{-1}); water yield (WY, mm); magnitude of the event relative to the initial baseflow (ΔQ; i.e., (Qmax-Qb)*100, %); relative length of the rising limb (RL, %) given by $RL=R_D/S_D$ *100 where R_D and S_D are the length (days) of the rising limb of the hydrograph and of the entire hydrograph, respectively; slope of the initial phase of the hydrograph falling limb (k, 1/day); runoff event duration (Rd, h); and the time from the previous runoff event (days). Finally, to describe NO_3 and TKN concentrations, the initial, maximum, and discharge-weighted mean concentrations of NO_3 and TKN measured during the events were included (NO_3C_0, NO_3Cmax, NO_3Cmean, $TKNC_0$, TKNCmax, TKNCmean, respectively; mg L^{-1}). The discharge-weighted mean concentration of the event was computed as total metal load divided by the total flow.

The hydrograph of the runoff events was separated in two components (event water and pre-event water) using EC, an environmental tracer widely used to determine the contribution of pre-event and event water to total event flow in catchments of varying sizes and under different climate conditions (Nolan and Hill 1990; Martínez-Santos et al., 2014). The main reasons for choosing this tracer were: on the one hand, the EC measurement is simple and inexpensive, which provides a suitable database for each runoff event and, on the other, the results of numerous studies that have used EC for hydrograph separation along with other tracers and/or more expensive isotope determination do not generally reveal any substantial differences in results, depending on the marker used (Cey et al., 1998; Pellerin et al., 2008).

The two-component mixing model was used to estimate the contribution of pre-event and event water to total flow, according to the following equation:

$$QtCt = QeCe + QpCp \tag{1}$$

where Q is discharge, C is the value of EC of the total event flow, pre-event and event water (t, p and e). As in other studies, EC value in the stream water prior to rainfall events was used to characterize the pre-event water, and EC value of rainfall to characterize event water.

The evolution of the contribution of pre-event (Qp) and event water (Qe) throughout the runoff events was also analyzed. For this purpose, Qp/Qe ratio was calculated to deduce whether the dynamics of NO_3 and TKN during runoff events are related to pre-event and event water contribution to total flow.

During the entire monitoring period, 173 runoff events were identified; 156 were sampled, the other 17 were missed because of technical problems with the equipment. In total, 102 events of varying magnitude and duration were selected for C-Q analysis in this study. Selection criteria used for hysteresis analysis of runoff events were that they had to have only one peak discharge with at least two samples collected on each limb of the hydrograph, and one sample at or close to peak discharge, because this was considered the minimum number of samples from which rotational direction could be identified. For each of the selected runoff events, C-Q NO_3 and TKN response were examined visually for the presence and direction of a hysteresis loop (by plotting concentration versus discharge) and classified into three types of responses: clockwise, anticlockwise and no

https://doi.org/10.5194/hess-2021-536
Preprint. Discussion started: 30 November 2021

Hydrology and Earth System Sciences
Open Access
Discussions

hysteresis. Events with a "figure of eight" hysteresis pattern were classified as a hysteresis response, with the direction depending on the succession of the peak concentration and peak discharge, in a similar way to (Bieroza and Heathwaite 2015).

Table 1. Characteristics of the runoff events (n=102) selected during the study

Variable		**Mean**	**Minimum**	**Maximum**	**V.C. (%)**
Antecedent conditions	Accumulated rainfall 7 days before the event (AP7d, mm)	35.18	0.60	124.40	81
	Accumulated rainfall 15 days before the event (AP15d, mm)	67.29	1.00	222.10	77
	Discharge at the beginning of the event (Qb, $m^3 s^{-1}$)	0.21	0.03	0.64	60
Event conditions	Rainfall amount (P, mm)	22.24	4.00	74.40	69
	Maximum 10-min rainfall intensity (IP10, mm h^{-1})	2.35	0.40	9.20	71
	Rainfall kinetic energy (KE, MJ ha^{-1})	3.16	0.52	10.49	74
	Peak discharge (Qmax, $m^3 s^{-1}$)	0.49	0.10	1.62	65
	Water yield (WY, mm)	40711.68	4097.01	190026	99
	Magnitude of the event (ΔQ, %)	165.57	17.65	853.33	92
	Relative length of the rising limb (RL, %)	33.63	11.63	64.35	38
	Slope of the initial phase of the hydrograph falling limb (k, 1/day)	-0.016	-0.053	-0.001	72
	Runoff event duration (Rd, h)	32.41	9.80	115.80	59
	Time from the previous runoff event (Δt, days)	9.87	0.00	169.38	212
NO_3 and TKN concentrations during the events	*NO_3*				
	Initial concentration (NO_3C_0, mg L^{-1})	5.41	3.11	12.61	27
	Maximum concentration (NO_3Cmax, mg L^{-1})	7.09	3.14	22.51	41
	Mean concentration (NO_3Cmean, mg L^{-1})	5.84	3.12	10.06	25
	TKN				
	Initial concentration ($TKNC_0$, mg L^{-1})	0.25	0.01	2.55	129
	Maximum concentration (TKNCmax, mg L^{-1})	1.47	0.08	9.41	96
	Mean concentration (TKNCmean, mg L^{-1})	0.6375	0.04	2.88	79
Hysteresis descriptors	*NO_3*				
	Hysteresis direction (ΔR, %)	-20.62	-93.00	60.00	151
	Hysteresis magnitude (ΔC, %)	3.86	-44.28	47.20	395
	TKN				
	Hysteresis direction (ΔR, %)	4.78	-72.00	69.00	513
	Hysteresis magnitude (ΔC, %)	66.15	-70.35	98.45	61

Following the methodology proposed by (Butturini et al., 2006; Butturini et al., 2008) the form, rotational patterns, and trends of NO_3 and TKN hysteresis loops were described by two parameters: ΔC and ΔR. ΔC (%) describes the relative changes in nitrogen (NO_3 or TKN) concentration and hysteresis trend, and is calculated using the following equation:

https://doi.org/10.5194/hess-2021-536
Preprint. Discussion started: 30 November 2021

Hydrology and Earth System Sciences
Discussions

$$\begin{cases} \frac{Cs-Cb}{Cmax} * 100 \text{ if } Cs > Cb \\ \frac{Cs-Cb}{Cb} * 100 \text{ if } Cs < Cb \end{cases} \quad (2)$$

where Cs and Cb are the nitrogen (NO_3 or TKN) concentrations at peak discharge and baseflow, respectively, and Cmax is the highest concentration measured in the stream during the runoff event. ΔC ranges from - 100 to 100%, where positive values indicate hysteresis loops following a positive trend with respect to the discharge, i.e., element flushing, and negative values indicate the opposite, i.e., solute dilution. ΔR (%) reflects the entire element dynamics during runoff events and provides information on the area (magnitude) and rotational (direction) pattern of the C-Q hysteresis. AR is calculated by the following equation:

$$\Delta R = R * Ah * 100 \quad (3)$$

where Ah is the area of the c-q hysteresis, estimated after standardizing discharges and concentrations to unit ($0 \leq Ah \geq 1$), and R describes the rotational pattern of the hysteresis. If the C-Q hysteresis is clockwise, R=1, and if it is anticlockwise, R=-1; for ambiguous or non-existent hysteresis, R=0. The parameter ΔR takes values from -100 to 100.

The variability of NO_3 and TKN hysteresis parameters, which can provide information on the dynamic of nitrogen availability and hydrological pathways, was examined by plotting ΔC versus ΔR. The plots can be divided in 9 regions (Butturini et al., 2008), each of which identifies a C-Q response type. For this, ΔC and ΔR parameters were classified in three distinct categories ("-1", "0", "1") using a threshold of 10%: $\Delta C < -10\%$ (element dilution); $-10\% \geq \Delta C \leq 10\%$ 0 (neutral); $\Delta C > 10\%$ (element release); $\Delta R < -10\%$ (anticlockwise loop); - 10%: $\Delta R < 10\%$ (no loop); $\Delta R > 10\%$ (clockwise loop). The 9 regions include the six C-Q hysteresis types proposed by Evans and Davies (1998) in addition to the simple lineal C-Q hysteresis (i.e., $\Delta R \approx 0$).

2.4 Statistical methods

To assess the main links between hysteresis descriptors (response variables) and the different hydro-meteorological and biogeochemical variables (explanatory variables) influencing these events, standard statistical methods were used, such as correlation and a redundancy analysis (RDA). The RDA output was represented in a biplot graph showing the correlation between explanatory and response variables given by the cosine of the angle between vectors. Thus, vectors pointing in roughly the same direction represent a positive correlation, while those pointing in opposite directions show a negative correlation.

Hydrology and Earth System Sciences
Open Access
Discussions

3 Results

3.1 Average characteristics of the rainfall-runoff events

The main characteristics of the runoff events selected for this study are summarized in Table 1. High variability in the variables defining the events was observed. Thus, the events varied greatly in terms of antecedent conditions (AP7d: 0.60 - 124.40 mm, AP15d: 1.00 - 222.10 mm, Qb: 0.03 - 0.64 $m^3 s^{-1}$), meteorological (P: 4.00 -74.40 mm, KE: 0.52 - 10.49 MJ ha^{-1}) and hydrological features (Qmax: 0.10 - 1.62 $m^3 s^{-1}$, ΔQ: 17.65 - 853.33%, Rd: 9.80 - 115.80 h), showing that those selected cover a wide range of meteorological and hydrological conditions. These events can be considered representative of the study period, because the meteorological and hydrological data of the events in this study cover virtually the entire range of rainfall, antecedent rainfall, and discharge from 5th to 95th percentile.

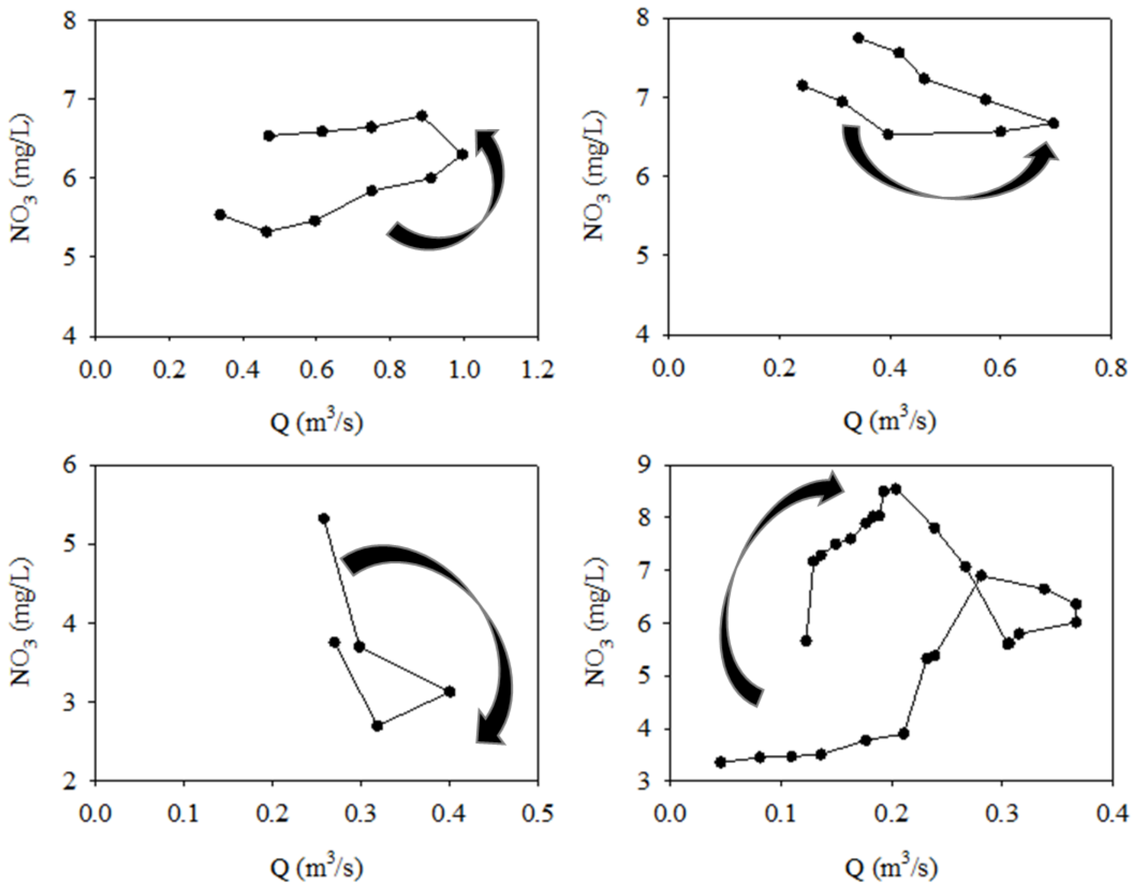

Figure 2: Examples of different types of NO_3 hysteresis patterns observed in the Corbeira catchment during the monitoring period.

https://doi.org/10.5194/hess-2021-536
Preprint. Discussion started: 30 November 2021

From the selected 102 rainfall-runoff events, 39 occurred in autumn, 30 in winter, 22 in spring and 11 in summer, so that about 70% were concentrated in the wettest period of the year (October-March). The magnitude of the runoff events tended to be high in autumn and winter when soil moisture is high, while in summer, when the catchment is dryer, the event magnitude tended to be lower (Rodríguez-Blanco et al., 2012a) (Figure 2). In the study area, the runoff events are usually linked to low-magnitude (mean P = 22.24 mm) and intensity (mean IP10 = 2.35 mm h^{-1}) rainfall events of long duration, although several with high magnitude (P > 50 mm) and intensity (IP 10 = 9.1 mm h-1) rainfall were registered during the study (Table 1). For most runoff events, an increase in NO3 and TKN concentrations were observed with discharge, but the magnitude of the increase varied markedly from one event to another. The mean and maximum N (NO3 and TKN) concentrations also varied among runoff events, especially for TKN; the maximum TKNCmean and TKNCmax values were two orders of magnitude higher than the respective minimum values (Table 1). The highest values of both elements were recorded during winter events (Figure 2).

3.2 Hysteresis direction and magnitude

The study of the relationship between the N (NO_3 and TKN) concentration and discharge revealed different hysteresis patterns for both elements in the catchment (Fig. 2 and Fig. 3). For NO_3, the parameter describing the change in concentration during the runoff events returned positive values ($\Delta C \geq 0\%$) in 64 events. These positive values show that NO_3 concentrations during the runoff events were mostly greater than the pre-event; but 35 of these events had ΔC values between 0% and 10%, indicating a slight shift in NO_3 concentrations (Butturini et al., 2008).

Based on hysteresis classification, 74% of the events exhibited anticlockwise hysteresis ($\Delta R < 0$), 21% clockwise hysteresis ($\Delta R > 0$) and the remaining 5% showed no or unclear hysteresis pattern ($\Delta R = 0$). However, it should be noted that approximately 13% of events had ΔR values between -10% and 10%, so in these cases it is considered that the hysteresis area is small (Butturini et al., 2008). NO_3 data are in all regions in the ΔC *vs.* ΔR unit plane (Fig. 3 up), however the most likely NO_3-Q responses are types 4 and 3, indicating dilution (negative ΔC) or flushing (positive ΔC) and anticlockwise hysteresis loops (negative ΔR).

Similar to NO_3, the TKN concentrations increased in almost all runoff events in respect of the baseflow values (positive ΔC in 93% of events), indicating that TKN flushing clearly predominates over dilution. In fact, the parameter describing the change in concentration during runoff events (ΔC) achieved negative values in only 7 runoff events (Fig. 3bottom), all of which were characterized by low rainfall. The rotational patterns of the TKN-Q hysteresis ranged from clockwise ($\Delta R > 0$) to anticlockwise ($\Delta R < 0$) (Fig. 3 bottom). About 53% of the events showed clockwise hysteresis, 39% anticlockwise hysteresis and the remaining 8% showed no or unclear hysteresis pattern; although it should be noted that 29% of the events showed small areas of the hysteresis loop (ΔR values comprised 10% and 10%). The hysteresis loops are located mainly in the regions 1, 2 and 3 (Fig. 3 bottom), suggesting a flushing (positive ΔC) and clockwise (positive ΔR) or anticlockwise loops (negative ΔR).

https://doi.org/10.5194/hess-2021-536
Preprint. Discussion started: 30 November 2021

Hydrology and Earth System Sciences
Open Access
EGU
Discussions

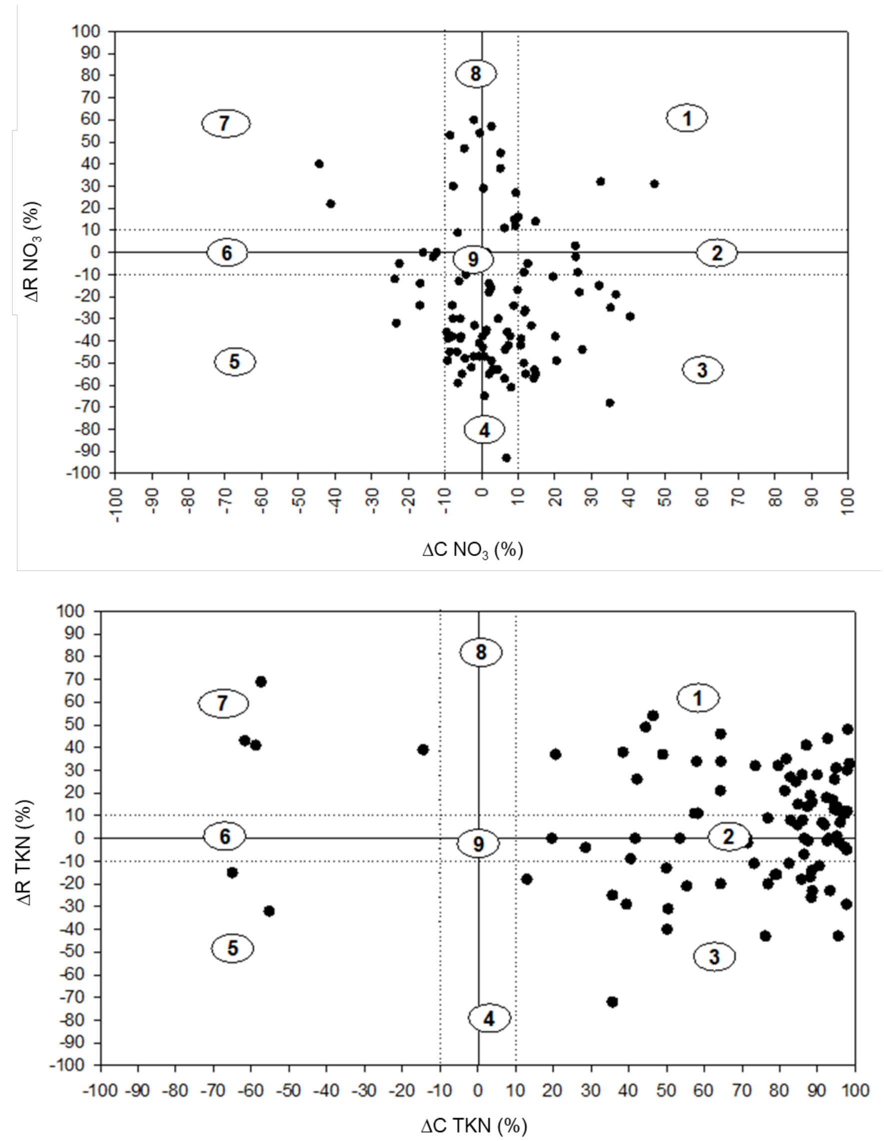

255 **Figure 3**: Representation of the C-Q hysteresis characteristics (ΔR, ΔC) of NO_3 (up) and TKN (bottom) in the unity plane.

3.3 C-Q hysteresis response controls

To identify the variables that might explain C-Q hysteresis patterns the relationships between hysteresis, hydrological and biogeochemical descriptors, variables were analyzed using a Pearson correlation matrix and an RDA analysis (Table 2 and Fig. 4). The results of the correlation analysis showed that the hysteresis direction and magnitude were more closely related to certain event characteristics than antecedent conditions (Table 2). Thus, of the representative variables of the event antecedent

Hydrology and Earth System Sciences
Discussions

conditions, significant correlations (negative sign) were only observed between Qb and the hysteresis magnitude parameter for NO_3 (r = -0.22, $p < 0.05$). The parameter describing information on the hysteresis direction for NO_3 (ΔR_{NO3}) showed negative correlations with P, IP10, KE, Qmax. On the contrary, a positive relationship was found between ΔR_{TKN} and P, KE, Qmax, WY and Rd. Regarding the parameters describing the change of concentration of NO_3 (ΔC_{NO3}) and TKN (ΔC_{TKN}), a positive correlation was found among these parameters (ΔC_{NO3}, ΔC_{TKN}) and the hydro-meteorological variables P, KE and ΔQ. An inverse relationship was found between ΔC_{TKN} and RL (r = - 0.23, $p < 0.01$) and K (r = - 0.31, $p < 0.01$). Finally, the concentrations during runoff events were not controlling factors for the direction of the hysteresis of NO_3 and TKN, but these variables (especially C_0) were controlling the hysteresis magnitude for NO_3 and TKN, although in different ways (Table 2). Thus, C_0 showed positive correlations with ΔC_{NO3} and negative with ΔC_{TKN}.

Table 2. Pearson correlation coefficients between hysteresis descriptors (ΔR and ΔC) and event characteristics. Values displayed in both indicates correlation is significant at 0.01 level and italics indicate correlation is significant at 0.05 level.

	Hysteresis direction (ΔR)		Hysteresis magnitude (ΔC)	
	NO_3	TKN	NO3	TKN
Antecedent conditions				
AP7d	-0.18	0.09	-0.19	-0.08
AP15d	-0.19	0.16	-0.19	-0.01
Qb	-0.14	0.12	*-0.22*	0.02
Event characteristics				
P	*-0.22*	**0.36**	**0.27**	**0.27**
IP10, mm h^{-1}	*-0.24*	0.00	0.05	*0.25*
KE	*-0.24*	**0.32**	*0.24*	0.31
Qmax	**-0.29**	**0.29**	-0.03	**0.28**
WY	-0.17	**0.38**	-0.08	0.04
ΔQ	-0.06	0.18	**0.29**	**0.35**
RL	0.03	-0.13	0.12	*-0.23*
K	0.10	0.17	-0.03	**-0.31**
Rd	-0.04	**0.37**	0.12	-0.09
Δt	0.08	0.03	**0.27**	0.05
Concentrations during the event				
C_0	-0.06	0.04	**0.40**	**-0.54**
Cmax	0.08	0.15	0.16	*0.25*
Cmean	-0.14	0.08	0.16	*0.24*

AP7d: accumulated rainfall 7 days before the event; AP15d: accumulated rainfall 15 days before the event; Qb: discharge at the beginning of the event; P: rainfall amount; IP10: maximum 10-min rainfall intensity; KE: rainfall kinetic energy; Qmax: peak discharge; WY: water yield; ΔQ: magnitude of the event; RL: relative length of the rising limb; k: slope of the initial phase of the hydrograph falling limb; Rd: runoff event duration, Δt: time from the previous runoff event (days); $C_{0:}$ initial concentration; Cmax: maximum concentration; Cmean: mean concentration.

The RDA analysis showed that the first two axes explained 82.3% of total variance in the descriptors in NO_3 and TKN hysteresis (ΔC_{NO3}, ΔC_{TKN}, ΔR_{NO3}, ΔR_{TKN}), accounting for the first and second canonical axes for 62.4% and 19.9%,

https://doi.org/10.5194/hess-2021-536
Preprint. Discussion started: 30 November 2021

respectively. ΔC_{TKN} and ΔR_{TKN} loaded positively in the first axis and pointed in the same direction as rainfall-runoff magnitude variables, indicating a positive relationship with these. ΔC_{TKN} and ΔC_{NO3} loaded negatively in the second axis and pointed in an opposite direction to k, suggesting that an inverse relationship exists between both variables. On the other hand, ΔR_{NO3} loaded negatively in the second axis and pointed in an opposite direction to P and Qmax, indicating that an inverse relationship occurs with these variables.

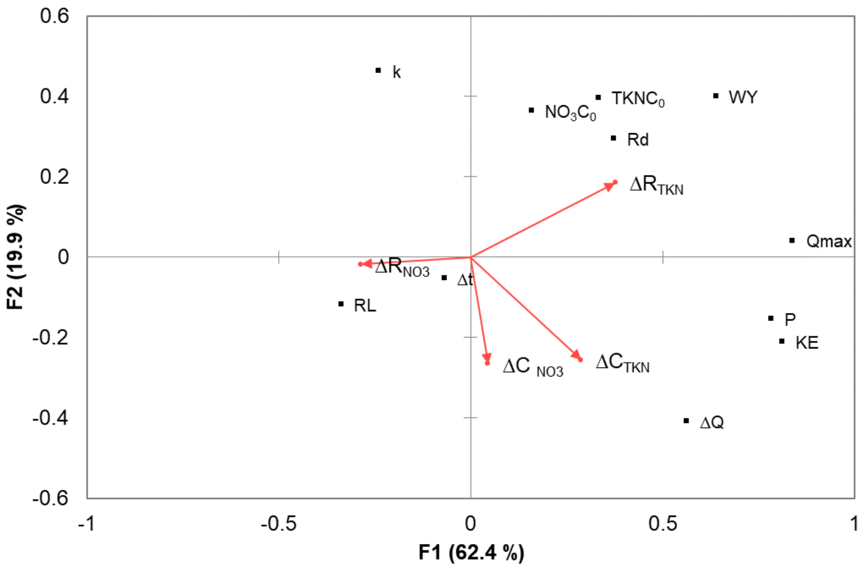

Figure 4 Redundancy analysis distance biplot showing ordinations of explanatory and response variables. P: rainfall amount;; KE: rainfall kinetic energy; Qmax: peak discharge; WY: water yield; ΔQ: magnitude of the event; RL: relative length of the rising limb; k: slope of the initial phase of the hydrograph falling limb; Rd: runoff event duration, Δt: time from the previous runoff event (days); NO_3 or TKN C_0: initial concentration; NO_3 or TKN Cmax: maximum concentration.

4 Discussion

4.1 Most frequent N runoff event response from hysteresis interpretation

In general, the NO_3 and TKN concentrations increased during runoff events in comparison to baseflow conditions, indicating the predominance of an enrichment response during runoff events and suggesting that the N delivery in the catchments is mainly controlled by diffuse sources. Nitrate concentrations in drinking water are restricted to 50 mg L^{-1} (11.3 N mg L^{-1}) (Directive 98/83/EC), and this limit was not exceeded for Corbeira. However, considering that in well-oxygenated surface waters, nitrate levels above 0.5-1.0 mg L^{-1} can pose a risk of water eutrophication (Camargo and Alonso, 2007) and that 2 mg L^{-1} is the threshold identified in the European Nitrogen Assessment as an appropriate target for establishing a river system

Hydrology and Earth System Sciences
Open Access
EGU
Discussions

in good ecological conditions, the data obtained (Table 1) indicate that the study area may be threatened by potential risk of eutrophication due to nitrogen concentration. This will clearly have important implications for compliance with water quality targets, and it must be borne in mind that the study area flows into the Abegondo-Cecebre reservoir, a very important source of drinking water for one of the largest cities in the northwest Iberian Peninsula.

Accretion pattern for NO_3 have been reported elsewhere, but they can be dominated by clockwise hysteresis (Winter et al., 2020) or anticlockwise as in our case (Dupas et al., 2016; Outram et al., 2016; Winter et al., 2021). The anticlockwise hysteresis means that contributors during the falling limb are richer in NO_3 than during the rising limb and has been frequently associated with nitrate transport via groundwater and subsurface flow (Butturini et al., 2006; Cerro et al., 2014; Outram et al., 2016). Groundwater, which dominates baseflow, contains low NO_3 concentrations in this catchment. Data supporting this interpretation are described in Rodríguez-Blanco et al., (2015), showing that NO_3 concentrations in summer (low-flow conditions dominated by groundwater) are lower (around 3.75 mg L^{-1}) than those measured in winter (5.67 mg L^{-1}). Therefore, it is reasonable to assume that, in this catchment, where the soils have high infiltration rates and much of streamflow comprises water leached through the soil profile, subsurface flow is a likely pathway delivering additional NO_3 during runoff events. In fact, in the events showing anticlockwise loops, the maximum NO_3 concentrations in the stream were registered after peak discharge (Figure 2) when the contribution of subsurface flow to streamflow is maximum, and then decreases as the subsurface recedes. This also suggests relatively higher NO_3 concentrations in the upper soil layers than deeper groundwater, arguably because of mineralization of organic matter and the mineral and organic fertilizer applied to agricultural soils in the catchment. While accretion with anticlockwise rotation was the dominant pattern for NO_3 in the study catchment, some events exhibited accretion patterns but with clockwise hysteresis (Fig. 2 and 3), indicating a higher NO_3 concentration in the rising limb of the hydrograph than in the falling limb. This pattern was mainly observed in small spring events occurred in 2008 and 2009 and could be attributed to the rapid transport of NO_3 from near-stream sources and/or hydrologically connected directly to the stream.

The above findings contrast with the general interpretations presented in several previous studies carried out in rural catchments (e.g., Bowes et al., 2015; Rose et al., 2018; D'Amario et al., 2021), which described exclusively NO_3 dilution processes linked to dilution of NO_3 concentrations in groundwater by surface runoff. However, in the study catchment, the dilution responses (with anticlockwise rotation ($\Delta C \leq 0\%$)) were only observed in certain runoff events recorded just after other events ($\Delta t <$ 1day). A possible reason for the initial dilution of the concentrations could be the preceding wetting of the catchment which favors the delivery of relatively low-nitrate water flushed to the stream from low-NO_3 concentration sources, such as direct rainfall to the stream and runoff from roads and paved area, as has been observed in other headwater streams (Poor and McDonnell 2007; Kato et al., 2009). Following the initial dilution, concentrations increased above pre-event values, reaching the highest NO_3 concentrations after maximum discharge. The return of NO_3 concentrations to the values before the rainfall-runoff event is especially slow in these events (Fig. 2) and NO_3 concentrations remain elevated for several days until streamflow returns to baseflow. This confirms once more the control exerted by subsurface flow on the NO_3 dynamics during runoff events in this catchment.

https://doi.org/10.5194/hess-2021-536
Preprint. Discussion started: 30 November 2021

Hydrology and Earth System Sciences
Discussions

Mechanisms responsible for TKN mobilization differ from those mobilizing NO_3. Thus, a clockwise accretion pattern for TKN concentration was dominant for most events, suggesting a delivery of TKN to the stream network via fast pathways from proximal sources, relatively easily connected to the stream as event runoff increases, with possible rapid exhaustion (Creed et al., 2015). Several studies have found organic nitrogen peaks on the rising limb, similar to our finding (Vanderbilt et al., 2003; Inamdar and Mitchell 2006; Rose et al., 2018). Thus, Vanderbilt et al., (2003) attributed this pattern to the flushing of decomposing leaf litter, while Inamdar and Mitchell (2006) reported that stream organic nitrogen was derived from throughfall. In the case of the Corbeira catchment, the TKN response was almost concurrent with discharge, so TKN may come from the eroded soil material delivered to the stream primarily by surface runoff, in a similar way to suspended sediment matter and particulate phosphorus (Rodríguez-Blanco et al., 2013; 2019). This is in accordance with findings from (D'Amario et al., 2021), who reported a dominance of clockwise patterns for TKN in Canadian catchments consisting of different types of land use due to the surface runoff of eroded soil particles. Although the dominant pattern for TKN concentrations is clockwise, some events showed anticlockwise trajectories. Hagedorn et al. (2000) attributed the delayed expression of organic nitrogen peaks to the mobilization of this element during its passage through the forest canopy and organic-rich topsoil. This pattern (anticlockwise) has also been linked to distant TKN source areas. However, given that the anticlockwise pattern for TKN in the study area was observed mainly during low magnitude events (20 of 26, $P < 16$ mm) recorded in spring and summer, it is highly unlikely to be the contribution from distal sources. Rather, given the event characteristics, the presence of anticlockwise hysteresis could provide evidence that more nitrogen, probably in dissolved form, passes through the soil and subsequently enters the stream by subsurface flow.

Hysteresis patterns may vary among events and antecedent soil moisture conditions are often recognized as an important factor in the response of different constituent concentrations among events, even when rainfall characteristics are approximately similar (Butturini et al., 2006; Baker and Showers, 2019). However, in this catchment, hysteresis direction and magnitude were better explained by event characteristics, such as rainfall, runoff, and discharge increase than by antecedent precipitation and baseflow. Thus, as rainfall gains in strength and intensity, and discharge increases during runoff events, the hysteresis magnitude value and nitrogen loss from the catchment also rise. The positive correlation between ΔC_{NO3} and Δt, i.e., the time elapsed since a preceding runoff event during which physical and biological processes operate to increase the store of available nitrogen, seems to point in the same direction. On the contrary, the events occurring under antecedent wetness conditions in the catchment have low nitrate concentrations in the soil water because it has already been washed by previous events (Rodríguez-Blanco et al., 2015). Several authors have highlighted the significant role played by rainfall-runoff events characteristic of hysteresis patterns (Chen et al., 2012; Lloyd et al., 2016). For example, (Chen et al., 2012) emphasized the role of the strength of the runoff event influencing the magnitude and rotation direction of the hysteresis patterns, whereas Lloyd et al., (2016) underlined the combined effect exerted by storm duration, maximum discharge during the runoff event and the time elapsing from the previous runoff events on controlling N hysteresis magnitude and rotation.

Understanding how the transference of N, or other elements, occurs is useful for implementing mitigation techniques to prevent water quality degradation (Bieroza et al., 2018). In this respect, the results acquired in this study underline the need to establish specific mitigation approaches for NO_3 and TKN. To minimize NO_3 losses, catchment management should focus on reducing N stores in the soil, whereas for protecting water quality against for TKN, measures decreasing surface runoff and hydrological connectivity between fields and the stream network are required. These guidelines would be applicable to other rural catchment water quality management decisions in the region.

5 Discussion

The results show the potential of high-frequency N concentration monitoring to advance our understanding of coupled hydrological and biogeochemical systems in the context of contrasting hydrometeorological conditions. The assessment of nitrogen concentration-Q relationships and their controlling factors has provided evidence of the different NO_3 and TKN dynamics during the runoff events, suggesting the presence of distinct delivery mechanisms and differences in dominant hydrological pathways. NO_3 behavior during the runoff events was dominated by anticlockwise hysteresis, indicating that subsurface flow is the main pathway to the stream. On the contrary, clockwise hysteresis prevailed in the TKN dynamic, pointing out that surface runoff is mainly responsible for the transport of TKN to the river.
The divergence dynamics observed between N components in the study area exemplifies the complexity and variability of NO_3 and TKN processes, highlighting the need to understand dominant hydrological pathways for the development of N-specific management plans to ensure that control measures are most effective at the catchment scale. Thus, the design of strategies to control surface runoff and hydrological connectivity will minimize TKN transport to the river.

Acknowledgements

This research was carried out within the projects REN2003-08143, funded by the Spanish Ministry of Education and Science, and PGIDIT05RAG10303PR and 10MDS103031PR, financed by the Xunta of Galicia.

References

Abbott, B.W., Bishop, K., Zarnetske, J.P., Minaudo, C., Chapin F.S., Drause, S., Hannah, D.M., Conner, L., Ellison, D., Godsey, S.E., Plont, S., Marçais, J., Kolbe, T., Huebner, A., Frei, R.J., Hampton, T., Gu, S., Buhman, M., Sayedi, S.S., Ursache, O., Chapin, M., Henderson, K.D., Pinay, G.: Human domination of the global water cycle absent from depictions and perceptions, Nat. Geosci., 12, 533-540, doi:10.1038/s41561-019-0374-y, 2019.

Aguilera, R. and Melack, J. M.: Concentration-discharge responses to storm events in Coastal California Watersheds, Water Resour. Res., 54, 407–424, doi:10.1002/2017WR021578, 2018.

APHA. 1998. Standard Methods for Examination of Water and Wastewater. APHA: Washington.

Ameijenda, C. Integrated management of water resources and its application to local planning of the Abegondo Cecebre 07/ENV/E/0826 LIFE+project. Spanis J Rural Develop., 1, 35-40, doi:10.5261/2010.ESP1.02, 2010

Baker, E. B. and Showers, W. J.: Hysteresis analysis of nitrate dynamics in the Neuse River, NC, 652, Scie. Totl Environ., doi:10.1016/j.scitotenv.2018.10.254, 2019.

Bieroza, M. Z. and Heathwaite, A. L.: Seasonal variation in phosphorus concentration-discharge hysteresis inferred from high-frequency in situ monitoring, J. Hydrol., 524, doi:10.1016/j.jhydrol.2015.02.036, 2015.

Bieroza, M. Z., Heathwaite, A. L., Bechmann, M., Kyllmar, K., and Jordan, P.: The concentration-discharge slope as a tool for water quality management, Scie. Total Environ., 630, 738–749, doi:10.1016/J.SCITOTENV.2018.02.256, 2018.

Bowes, M. J., Jarvie, H. P., Halliday, S. J., Skeffington, R. A., Wade, A. J., Loewenthal, M., Gozzard, E., Newman, J. R., and Palmer-Felgate, E. J.: Characterising phosphorus and nitrate inputs to a rural river using high-frequency concentration-flow relationships, Scie. Total Environn., 511, doi:10.1016/j.scitotenv.2014.12.086, 2015.

Burns, D. A., Pellerin, B. A., Miller, M. P., Capel, P. D., Tesoriero, A. J., and Duncan, J. M.: Monitoring the riverine pulse: Applying high-frequency nitrate data to advance integrative understanding of biogeochemical and hydrological processes, WIRES Water, 6, doi:10.1002/wat2.1348, 2019.

Butturini, A., Francesc, G., Jérôme, L., Eusebi, V., and Francesc, S.: Cross-site comparison of variability of DOC and nitrate c-q hysteresis during the autumn-winter period in three Mediterranean headwater streams: A synthetic approach, Biogeochemistry, 77, doi:10.1007/s10533-005-0711-7, 2006.

Butturini, A., Alvarez, M., Bernał, S., Vazquez, E., and Sabater, F.: Diversity and temporal sequences of forms of DOC and NO3- discharge responses in an intermittent stream: Predictable or random succession?, J. Geophys. Res. Biogeosci., 113, doi:10.1029/2008JG000721, 2008.

Camargo, J.A., Alonso, A.: Contaminación por nitrógeno inorgánico en los ecosistemas acuáticos: problemas medioambientales, criterios de calidad del agua, e implicaciones del cambio climático, Ecosistemas, 16, 98-110, 2007.

Cerro, I., Sanchez-Perez, J. M., Ruiz-Romera, E., and Antigüedad, I.: Variability of particulate (SS, POC) and dissolved (DOC, NO_3) matter during storm events in the alegria agricultural watershed, Hydrol. Process., 28, doi:10.1002/hyp.9850, 2014.

Cey, E.E., Rudolph, D.L., Parkin, G.W., Aravena, R.: Quantifying groundwater discharge to a small perennial stream in southern Ontario, Canada. J. Hydrol., 210, 21–37, doi:10.1016/S0022-1694(98)00172-3, 1998.

Chen, N., Wu, J., and Hong, H.: Effect of storm events on riverine nitrogen dynamics in a subtropical watershed, southeastern China, Scie. Total Environ., 431, doi:10.1016/j.scitotenv.2012.05.072, 2012.

Creed, I. F., Mcknight, D. D. M., Pellerin, B. A., Green, M. B., Bergamaschi, B. A., Aiken, G. R., et al. (2015). The river as a chemostat: Fresh perspectives on dissolved organic matter flowing down the river continuum. Can. J. Fish. Aquat. Sci., 14, 1–1285, doi:10.1139/cjfas-2014-0400

D'Amario, S. C., Wilson, H. F., and Xenopoulos, M. A.: Concentration-discharge relationships derived from a larger regional dataset as a tool for watershed management, Ecol. Appl., doi:10.1002/eap.2447, 2021.

Dupas, R., Jomaa, S., Musolff, A., Borchardt, D., and Rode, M.: Disentangling the influence of hydroclimatic patterns and agricultural management on river nitrate dynamics from sub-hourly to decadal time scales, Scie. Total Environ., 571, doi:10.1016/j.scitotenv.2016.07.053, 2016.

EC (European Comision) 2019. Informe de la comisión al parlamento europeo y al consejo sobre la aplicación de la directiva marco sobre el agua (2000/60/ce) y la directiva sobre inundaciones (2007/60/ce) segundos planes hidrológicos de cuenca primeros planes de gestión del riesgo de inundación. SWD 42. 234 pp.

EEA, 2018. European waters -- Assessment of status and pressures 2018. 90 pp.

Eludoyin, A. O., Griffith, B., Orr, R. J., Bol, R., Quine, T. A., and Brazier, R. E.: An evaluation of the hysteresis in chemical concentration–discharge (C–Q) relationships from drained, intensively managed grasslands in southwest England, Hydrol. Scie. J., 62, 1243–1254, doi:10.1080/02626667.2017.1313979, 2017.

EU (European Union): 1998, Directive 98/83/CE relative to human drinking water quality, Official Journal of European Communities L330.

EU (European Union): 2000, Directive 2000/60/CE of the European Parliament and of the Council establishing a framework for community action in the field of water policy, Official Journal of European Communities L327.

Evans, C., and Davies, T. D.: Causes of concentration/discharge hysteresis and its potential as a tool for analysis of episode hydrochemistry, Water Resour. Res., 34(1), 129–137, doi: 10.1029/97WR01881, 1998.

Hagedorn, F., Schleppi, P., Waldner, P., and Flühler, H.: Export of dissolved organic carbon and nitrogen from Gleysol dominated catchments - The significance of water flow paths, Biogeochemistry, 50, doi:10.1023/A:1006398105953, 2000.

IGME (Instituto Tecnológico Geominero de España), 1981. Mapa Geológico de España, 1:50,000. Hoja 45. Betanzos. Spain.

Inamdar, S. P. and Mitchell, M. J.: Hydrologic and topographic controls on storm-event exports of dissolved organic carbon (BOC) and nitrate across catchment scales, Water Resour. Res., 42, doi:10.1029/2005WR004212, 2006.

Kato, T., Kuroda, H., and Nakasone, H.: Runoff characteristics of nutrients from an agricultural watershed with intensive livestock production, J. Hydrol., 368, doi:10.1016/j.jhydrol.2009.01.028, 2009.

IUSS Working Group WRB. 2014. World Reference Base for Soil Resources. 2014. International soil classification system for naming soils and creating legends for soil maps. World Soil Resources Reports. No 106. Rome. FAO.

Kaushal, S. S. and Lewis, W. M.: Patterns in the chemical fractionation of organic nitrogen in Rocky Mountain streams, Ecosystems, 6, doi:10.1007/s10021-003-0175-3, 2003.

Knapp, J. L. A., von Freyberg, J., Studer, B., Kiewiet, L., and Kirchner, J. W.: Concentration-discharge relationships vary among hydrological events, reflecting differences in event characteristics, Hydrol. Earth Syst. Sci., 24, 2561–2576, doi:10.5194/HESS-24-2561-2020, 2020.

Linsley, R.K., Kohler, M.A., Paulhus, J.C. 1949. Applied hydrology. McGraw-Hill Book Co., New York.

Lloyd, C. E. M., Freer, J. E., Johnes, P. J., and Collins, A. L.: Using hysteresis analysis of high-resolution water quality monitoring data, including uncertainty, to infer controls on nutrient and sediment transfer in catchments, Sci. Total Environ., 543, doi:10.1016/j.scitotenv.2015.11.028, 2016.

Martínez-Santos, M., Antigüedad, I., and Ruiz-Romera, E.: Hydrochemical variability during flood events within a small forested catchment in Basque Country (Northern Spain), Hydrol. Process., 28, doi:10.1002/hyp.10011, 2014.

Meybeck, M.: Looking for water quality, Hydrol. Process., 19, 331-338, doi:10.1002/hyp.5778, 2005.

Nolan, K. M. and Hill, B. R.: Storm-runoff generation in the Permanente Creek drainage basin, west central California - An example of flood-wave effects on runoff composition, J. Hydrol., 113, doi:10.1016/0022-1694(90)90183-X, 1990.

Outram, F. N., Cooper, R. J., Sünnenberg, G., Hiscock, K. M., and Lovett, A. A.: Antecedent conditions, hydrological connectivity and anthropogenic inputs: Factors affecting nitrate and phosphorus transfers to agricultural headwater streams, Sci. Total Environ., 545–546, doi:10.1016/j.scitotenv.2015.12.025, 2016.

Pellerin, B.A., Wollheim, W.M., Feng, X., Vörsmarty, C.J.: The application of electrical conductivity as a tracer for hydrograph separation in urban catchments. Hydrol. Process., 22, 1810-1818, doi:10.1002/hyp.6786

Poor, C. J. and McDonnell, J. J.: The effects of land use on stream nitrate dynamics, J. Hydrol., 332, doi:10.1016/j.jhydrol.2006.06.022, 2007.

Ramos, T. B., Gonçalves, M. C., Branco, M. A., Brito, D., Rodrigues, S., Sánchez-Pérez, J. M., Sauvage, S., Prazeres, Â., Martins, J. C., Fernandes, M. L., and Pires, F. P.: Sediment and nutrient dynamics during storm events in the Enxoé temporary river, southern Portugal, catena, 127, doi:10.1016/j.catena.2015.01.001, 2015.

Rodríguez-Blanco, M. L., Taboada-Castro, M. M., and Taboada-Castro, M. T.: Rainfall-runoff response and event-based runoff coefficients in a humid area (northwest Spain), Hydrol. Sci. J., 57, doi:10.1080/02626667.2012.666351, 2012.

Rodríguez-Blanco, M. L., Taboada-Castro, M. M., and Taboada-Castro, M. T.: Phosphorus transport into a stream draining from a mixed land use catchment in Galicia (NW Spain): Significance of runoff events, J. Hydrol., 481, doi:10.1016/j.jhydrol.2012.11.046, 2013.

Rodríguez-Blanco, M. L., Taboada-Castro, M. M., Taboada-Castro, M. T., and Oropeza-Mota, J. L.: Relating nitrogen export patterns from a mixed land use catchment in NW Spain with rainfall and streamflow, Hydrol. Process., 29, doi:10.1002/hyp.10388, 2015.

Rodríguez-Blanco, M. L., Taboada-Castro, M. M., and Taboada-Castro, M. T.: An overview of patterns and dynamics of suspended sediment transport in an agroforest headwater system in humid climate: Results from a long-term monitoring, Scie. Total Environ., 648, doi:10.1016/j.scitotenv.2018.08.118, 2019.

Rodríguez-Blanco, M. L., Taboada-Castro, M. M., and Taboada-Castro, M. T.: An assessment of the recent evolution of the streamflow in a near-natural system: A case study in the headwaters of the mero basin (galicia, Spain), Hydrol., 7, doi:10.3390/hydrology7040097, 2020.

Rose, L. A., Karwan, D. L., and Godsey, S. E.: Concentration–discharge relationships describe solute and sediment mobilization, reaction, and transport at event and longer timescales, Hydrol. Process., 32, 2829–2844, doi:10.1002/hyp.13235, 2018.

Vanderbilt, K. L., Lajtha, K., and Swanson, F. J.: Biogeochemistry of unpolluted forested watersheds in the Oregon Cascades: Temporal patterns of precipitation and stream nitrogen fluxes, Biogeochemistry, 62, doi:10.1023/A:1021171016945, 2003.

https://doi.org/10.5194/hess-2021-536
Preprint. Discussion started: 30 November 2021

Vörösmarty, C. J., McIntyre, P. B., Gessner, M. O., Dudgeon, D., Prusevich, A., Green, P., Glidden, S., Bunn, S. E., Sullivan, C. A., Liermann, C. R., Davies, P. M.: Global threats to human water security and river biodiversity, Nature, 467, 555-561, doi: 10.1038/nature09440, 2010.

Winter, C., Lutz, S. R., Musolff, A., Kumar, R., Weber, M., and Fleckenstein, J. H.: Disentangling the impact of catchment heterogeneity on nitrate export dynamics from event to long-term time scales, Water Resour. Res., 57, doi:10.1029/2020WR027992, 2021.